do not include our systematic error of 15 percent or any estimate of the error caused by any expected partial incorrectness of our assumptions.

[9]This equation has been changed by a factor of 4, by which it was incorrect in the original.

[10]C. de Vries, R. Hofstadter, and R. Herman, Phys. Rev. Letters 8, 381 (1962).

[11]H. Shwe, F. M. Smith, and W. H. Barkas, Bull. Am. Phys. Soc. 7, 282 (1962).

[12]J. J. Sakurai, Phys. Rev. Letters 7, 355 (1961).

POSSIBLE RESONANCES IN THE $\Xi\pi$ AND $K\bar{K}$ SYSTEMS*

L. Bertanza,† V. Brisson,‡ P. L. Connolly, E. L. Hart, I. S. Mittra,|| G. C. Moneti,⊥ R. R. Rau, N. P. Samios, I. O. Skillicorn,** and S. S. Yamamoto
Brookhaven National Laboratory, Upton, New York

and

M. Goldberg, L. Gray, J. Leitner, S. Lichtman, and J. Westgard
Syracuse University, Syracuse, New York

(Received July 2, 1962)

The purpose of this note is to report the existence of marked departures from phase space in the effective-mass distributions for the $\Xi\pi$ and $K\bar{K}$ states. We present evidence that, in about 25% of the events observed, the $\Xi\pi$ state results from the decay of a resonant state (Ξ^*) with a mass of 1535 MeV and a full width of <35 MeV. The observed anomaly in the $K\bar{K}$ effective-mass distribution is possibly open to different interpretations. If we assume it to be due to the decay of a resonant state K^*, we find that M_{K^*} = 1020 MeV, and that it has a full width of 20 MeV. However, it may also be possible to explain the effect as due to S-wave $K\bar{K}$ scattering. These results, as well as preliminary evidence concerning the properties of the Ξ^* and K^*, are discussed below.

The data for this experiment were obtained in an exposure of the BNL 20-in. hydrogen bubble chamber at the Brookhaven AGS. Details of the exposure and beam have been previously discussed.[1] Data were obtained both at 2.24 and 2.5 BeV/c. The sample reported on here consists of 79 $\Xi\pi$ and 37 $K\bar{K}$ combinations from the following production modes:

$$K^- + p \to \Xi^- + \pi^+ + K^0 \quad (1a)$$
$$\Xi^- + \pi^0 + K^+ \quad (1b)$$
$$\Xi^0 + \pi^- + K^+ \quad (1c)$$
$$\Xi^0 + \pi^0 + K^0 \quad (1d)$$
$$\to \Lambda + \bar{K}^0 + K^0 \quad (2a)$$
$$\Lambda + K^- + K^+ \quad (2b)$$

All events were measured and analyzed using the BNL TRED-KICK system. Except for Reaction (1d),[2] we believe the contamination from other topologically similar event types to be negligible.

For each of the above reaction types, the distributions of the square of the effective mass, defined by

$$M_{\rm eff}^2 = [(\sum_i E_i)^2 - (\sum_i \vec{p}_i)^2],$$

were obtained. The results are shown in Figs. 1 and 2 in the form of Dalitz plots with $M_{\rm eff}^2$ distributions projected onto the appropriate axes. The departures from the phase-space predictions are 3 standard deviations for the $\Xi\pi$ and 2.5 standard deviations for the $K\bar{K}$ effective-mass-squared distribution. This estimate of error is based on the square root of the total number of events in the bins containing the peaks in the $\Xi\pi$ and the $K\bar{K}$ Dalitz plots (see Figs. 1 and 2). Note

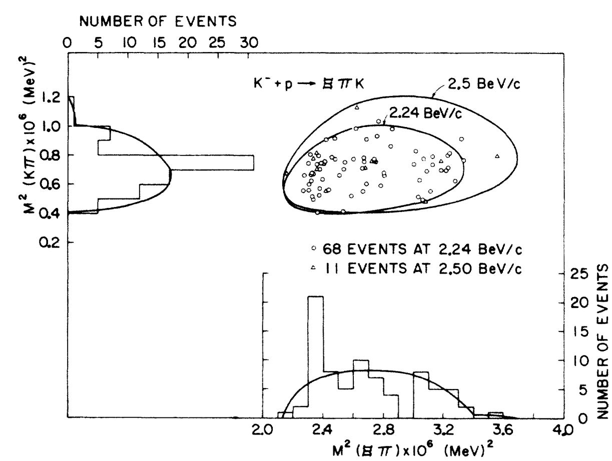

FIG. 1. The Dalitz plot for the channel $\Xi\pi K$ projected on the $M^2(K\pi)$ and the $M^2(\Xi\pi)$ axes. The solid curves on the projections are the invariant phase-space curves normalized to the total number of events.

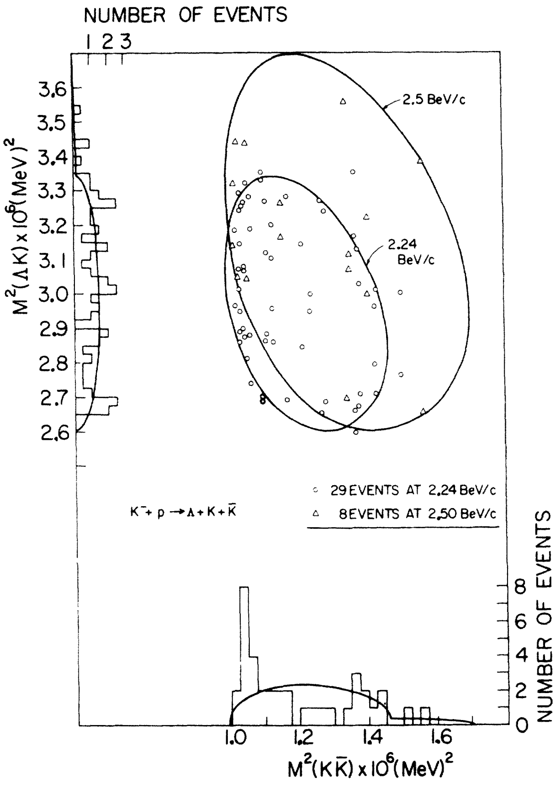

FIG. 2. The Dalitz plot for the channel $\Lambda K\bar{K}$ projected on the $M^2(K\bar{K})$ and $M^2(\Lambda K)$ axes. The solid curves on the projections are the invariant phase-space curves normalized to the total number of events.

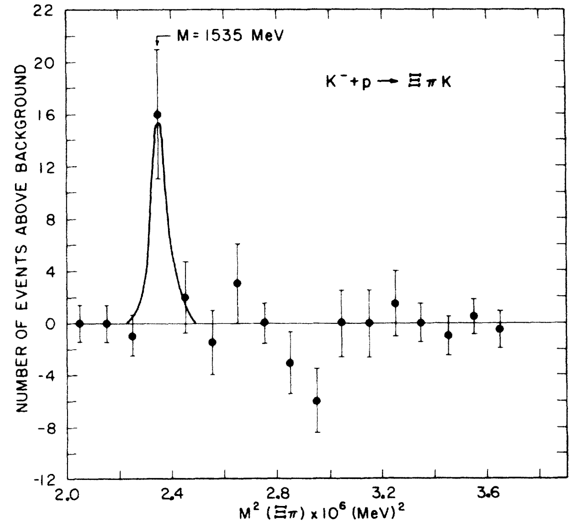

FIG. 3. The (effective mass)^2 distribution for $\Xi^-\pi$ from the channels $\Xi^-\pi^+K^0$ and $\Xi^-\pi^0K^+$ for those events above phase space.

that the phase-space plots are normalized to the total number of events in the Dalitz plots.[3] We discuss these results for the $\Xi\pi$ and $K\bar{K}$ systems separately.

In Fig. 1, two clusters of events are clearly visible. The first at $M_{\mathrm{eff}}^2(\Xi\pi) = 2.35$ BeV^2 corresponds to the proposed Ξ^*, and the second at $M_{\mathrm{eff}}^2(K\pi) = 0.75$ BeV^2 corresponds to the K^*. From the orientation of the Dalitz plot, it is clear that whereas the K^* resonance cannot produce a peak in the $M_{\mathrm{eff}}^2(\Xi\pi)$ distribution, the Ξ^* strongly influences the $M_{\mathrm{eff}}^2(K\pi)$ distribution as is evidenced by its asymmetry. A detailed study of interference effects is precluded by the relatively small number of events. In order to best obtain the mass and width of the Ξ^* peak, we have plotted in Fig. 3 the $M_{\mathrm{eff}}^2(\Xi\pi)$ distribution after subtract- the phase-space contribution. From this distribution we obtain $M_{\Xi^*} = 1535$ MeV and $\Gamma < 35$ MeV.[4] Some information concerning the isotopic spin of the Ξ^* can be obtained by examining the decay ratios,

$$R_1 = \Xi^* \to \Xi^-\pi^+ / \Xi^* \to \Xi^0\pi^0$$

and

$$R_2 = \Xi^* \to \Xi^0\pi^- / \Xi^* \to \Xi^-\pi^0.$$

Taking only those events which lie in the Ξ^* peak, and requiring for R_1 that the associated K_1^0 is observed, and for R_2 that the Λ from $\Xi^{0,-}$ decay is observed, we find $R_1 = 5/0$; $R_2 = 3/2$. These values should be compared with the expected $R_1 = R_2 = 2$ for $I_{\Xi^*} = 1/2$ and $R_1 = R_2 = 1/2$ for $I_{\Xi^*} = 3/2$, favoring a Ξ^* isotopic spin of 1/2. A similar indication is obtained from the observed production ratio, R_3, of Reactions (1a) and (1b). If the Ξ^* had $I = 3/2$, the above reactions could proceed only via the $I = 1$ channel and the expected value of R_3 would be 1/2. The observed ratio based on the subsample of events in which the Λ from Ξ^- was observed in $R_3 = 10/2$.[5]

Information on the spin, J_{Ξ^*}, is obtained from a study of the (folded) up-down Ξ^* decay distributions, i.e., the distribution of the Ξ^* decay pion, $\hat{q}_\pi$, in the Ξ^* center-of-mass frame, with respect to the normal, $\hat{n}$, to the Ξ^* production plane. If the Ξ^* spin were >1/2 and the Ξ^* were polarized in production, the distribution would be anisotropic. The observed distribution for the events in the peak give

$$(|\hat{n}\cdot\hat{q}_\pi| > 0.5)/(|\hat{n}\cdot\hat{q}_\pi| < 0.5) = 15/5.$$

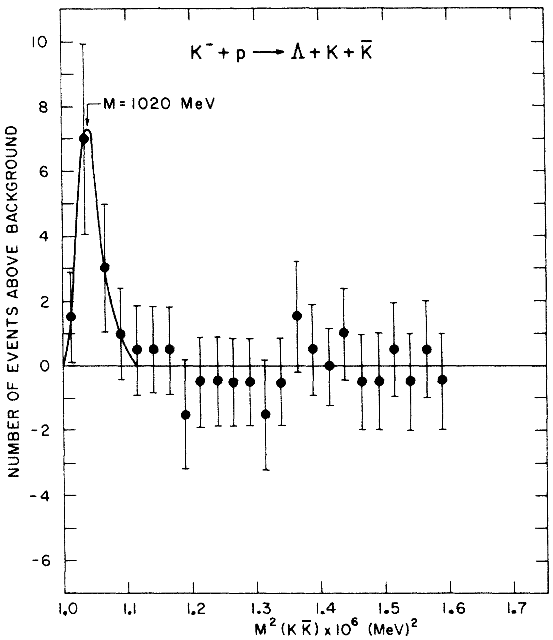

FIG. 4. The (effective mass)^2 distribution for $K\bar{K}$ from the channel $\Lambda K\bar{K}$ for those events above phase space.

This result is two standard deviations away from isotropy suggesting $J_{\Xi^*} > 1/2$.

We now discuss the $K\bar{K}$ system. Figure 2 clearly shows a grouping in the region $M_{\text{eff}}^2(K\bar{K}) = 1.05$ BeV^2 and no significant departure from phase space in the $M_{\text{eff}}^2(\Lambda K)$ distribution. Assuming that this peak is not due to a statistical fluctuation,[3] there exist the possibilities that it is a $K\bar{K}$ resonance or an S-wave final-state $K\bar{K}$ interaction. To study the $K\bar{K}$ peak more carefully we have replotted the M_{eff}^2 distribution after subtracting the phase-space contribution (see Fig. 4). From this plot we find $M_{K^*} = 1020$ MeV and $\Gamma_{K^*} = 20$ MeV. Because the departure from phase space occurs so close to the threshold, there exists the possibility that it is due to S-wave final-state interaction between the K and $\bar{K}$. Using the simplest form of effective range formalism to describe the K-$\bar{K}$ scattering, the appropriate distribution of $K\bar{K}$ effective masses becomes

$$f(M_{\text{eff}}) = \text{phase space}/[k^2 + (-a^{-1} + \tfrac{1}{2}r_0 k^2)^2],$$

where $k^2 = \frac{1}{4}M_{\text{eff}}^2 - M_K^2$. A comparison of the observed data with the distribution of $M_{\text{eff}}^2(K\bar{K})$ for two values of the scattering length, a, and effective range, r_0, is shown in Fig. 5. We find that a good fit can be obtained only for positive scattering lengths, corresponding to bound $K\bar{K}$ states, and for large values of r_0. Statistics are too poor, however, to draw any conclusion other than that the peak is consistent with both a $K\bar{K}$ resonance and a S-wave interaction.

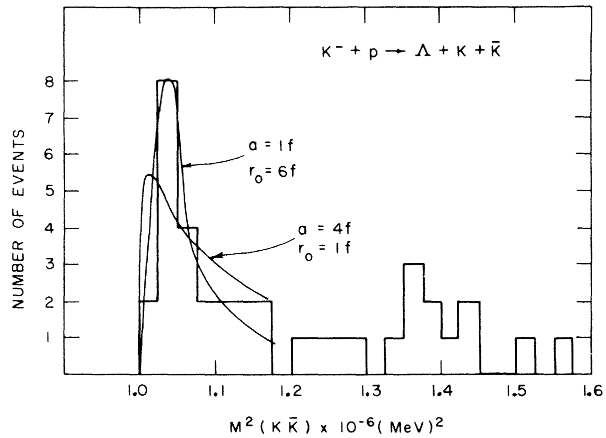

FIG. 5. The (effective mass)^2 distribution for $K\bar{K}$ from the channel $\Lambda K\bar{K}$. The solid curves show the distributions expected from the effective range approximation for $a = 1$, $r_0 = 6$, and $a = 4$, $r_0 = 1$.

We should like to acknowledge the cooperation of the AGS staff and the 20-in. hydrogen chamber crew for aid in obtaining the film.

---

*Work performed under the auspices of the U. S. Atomic Energy Commission. Research supported in part by the Office of Naval Research and the National Science Foundation.

†On leave of absence from the Istituto Nazionale di Fisica Nucleare, Pisa, Italy and The University of Pisa, Pisa, Italy.

‡On leave of absence from Ecole Polytechnique, Paris, France.

‖On leave of absence from Panjab University, Panjab, India.

⊥On leave of absence from the Istituto Nazionale di Fisica Nucleare, Rome, Italy and The University of Rome, Rome, Italy.

**On leave of absence from Imperial College, London, England.

[1]L. Bertanza, V. Brisson, P. L. Connolly, E. L. Hart, I. S. Mittra, G. C. Moneti, R. R. Rau, N. P. Samios, I. O. Skillicorn, S. S. Yamamoto, M. Goldberg, L. Gray, J. Leitner, S. Lichtman, and J. Westgard (to be published).

[2]Such events are detectable if they appear as double V productions in which (a) the Λ does not fit to the primary vertex, (b) the K^0 fits the primary vertex, and (c) no fit to the two-body kinematics is observed. Five such events were found.

[3]An analysis has been made of the effective-mass-

squared distributions of the $\Xi\pi$ and $K\bar{K}$ systems by means of the χ^2 test. The probabilities that the observed distributions originate from their corresponding phase-space distributions are <0.0001 for the $\Xi\pi$ system and <0.01 for the $K\bar{K}$ system. The large χ^2 values arise mainly from the single peaks appearing in each curve.

[4]For both the $\Xi\pi$ and $K\bar{K}$ systems the mass resolution is about ±3 MeV. This resolution has been estimated from the distribution of Λ masses found when the pion and proton from the Λ decay have been fitted to the production vertex.

[5]No subtraction of background has been made in the derivation of these ratios.

REGGE POLE MODEL FOR HIGH-ENERGY p-p AND $\bar{p}$-p SCATTERING

F. Hadjioannou, R. J. N. Phillips,* and W. Rarita,†
CERN, Geneva, Switzerland
(Received July 27, 1962)

The p-p data from 3 to 30 GeV/c seem to fit the assumption of a single vacuum Regge pole trajectory[1] (which we label P) and have been analyzed in these terms.[2-5] However, two more trajectories must in fact be important in this region: the ω trajectory to give the big difference between p-p and $\bar{p}$-p scattering, and a second vacuum trajectory (lablled P') to keep the p-p total cross section roughly constant.[6] (Igi[7] has already established the presence of P' from π-N dispersion relations.) Other known trajectories seem less important; the ρ trajectory gives differences between p-p and n-p scattering, but these are small.[2]

It is important to know if these extra poles spoil the one-pole analysis. We present here a realistic model of p-p and $\bar{p}$-p scattering, using the P, P', and ω trajectories, which fits many aspects of the data. This model suggests that one-pole analyses need certain corrections but remain qualitatively valid.

We first assume the scattering is dominated by the spin-averaged amplitude; this is reasonable, at least in the diffraction peak, and leaves a scalar problem. (A complete spinor treatment[8,9] introduces some modifications to be discussed later.) The amplitude contains terms of the usual form

$$T=\beta(t)P_\alpha(\cos\Theta_t)[1\pm\exp(-i\pi\alpha)]/\sin\pi\alpha, \qquad (1)$$

where $\alpha(t)$ is the corresponding trajectory, t is the invariant momentum transfer squared, P_α is the Legendre function, Θ_t is the scattering angle in the crossed channel, and $\beta(t)$ is the residue function. The signature ± is + for P and P', and - for ω. The p-p and $\bar{p}$-p amplitudes have the forms

$$T\begin{pmatrix}p\text{-}p\\ \bar{p}\text{-}p\end{pmatrix}=T_P+T_{P'}\pm T_\omega \qquad (2)$$

in an obvious notation.

From $\beta(t)$ we factor out the statistical weight $(2\alpha+1)$, a factor α to remove[8] "ghost" singularities at $\alpha=0$ for P and P', and the threshold dependence[8,10] $(t-4m^2)^\alpha/(4m^2)^\alpha$ where m is the nucleon mass; any remaining t dependence is ignored. The choice of units to make the threshold term dimensionless is not trivial, for it affects the t dependence. We note that the factor $(2\alpha+1)$ also serves to remove a singularity in P_α at $\alpha=-\frac{1}{2}$. The ω term has no ghost at $\alpha=0$, but we keep the factor α for symmetry; it also helps to fit the data, as explained later.

We now use the asymptotic form of P_α, write $\cos\Theta_t=(2s-4m^2+t)/(t-4m^2)$ where s is the invariant energy squared, and neglect t compared to s. Each pole term becomes

$$T=B\alpha(2\alpha+1)2^\alpha\frac{\Gamma(\alpha+\frac{1}{2})}{\Gamma(\alpha+1)}\frac{1\pm\exp(-i\pi\alpha)}{\sin\pi\alpha}\left(\frac{s-2m^2}{2m^2}\right)^\alpha, \qquad (3)$$

where B is a constant and Γ is the gamma function. Note that $(s-2m^2)/2m=E_L$, the total proton laboratory energy.

We assume the P trajectory is a straight line between $\alpha_P=1$ at $t=0$ and $\alpha_P=0$ at $t=-1$ (GeV/c)^2, as suggested by the one-pole analysis; we restrict ourselves to this range of t. Since the P' and ω contributions to the p-p total cross section are to cancel, their trajectories and residues are equal at $t=0$; we continue this symmetry for $t<0$ by choosing these trajectories to coincide on a straight line parallel to the P trajectory. The intercept at $t=0$ is taken to be 0.5 from Igi's work[7]; this value also seems consistent with the variations of total cross sections in the N-N, $\bar{N}$-N, π-N, K-N, and $\bar{K}$-N systems. The numerical coefficients are chosen in the ratio $B_P:B_{P'}:B_\omega=0.45:1:1$ for an approximate fit to